Integrated sensing layer of bacterial cellulose and polyethyleneimine to achieve high sensitivity of ST-cut quartz surface acoustic wave formaldehyde gas sensor

J L Wang[a], Y J Guo[a,*], G D Long[a], Y L Tang[b,*], Q B Tang[a], X T Zu[c], J Y Ma[d], B Du[d], H Torun[e], Y Q Fu[e,*]

[a] School of Physics, University of Electronic Science and Technology of China, Chengdu, 610054, P. R. China

[b] School of Physical Science and Technology, Southwest Jiaotong University, Chengdu, 610031, P. R. China

[c] Institute of Fundamental and Frontier Sciences, University of Electronic Science and Technology of China, Chengdu, 610054, P. R. China

[d]Sichuan Institute of Piezoelectric and Acousto-Optic Technology, Chongqing, 400060, P. R. China

[e] Faculty of Engineering & Environment, University of Northumbria, Newcastle upon Tyne, NE1 8ST, UK

*Corresponding authors and E-mail addresses:

Prof. Yuanjun Guo (guoyuanjun@uestc.edu.cn); Prof. Richard Yongqing Fu (richard.fu@northumbria.ac.uk); associate Prof. Yongliang Tang (tyl@swjtu.edu.cn).

Abstract:

Surface acoustic wave (SAW)-based formaldehyde gas sensor using bi-layer nanofilms of bacterial cellulose (BC) and polyethyleneimine (PEI) was developed on an ST-cut quartz substrate using sol-gel and spin coating processes. BC nanofilms significantly improve the sensitivity of PEI films to formaldehyde gas, and reduces response and recovery times. The BC films have superfine filamentary and fibrous network structures, which provide a large number of attachment sites for the PEI particles. Measurement results obtained using *in situ* diffuse reflectance Fourier transform infrared spectroscopy showed that the primary amino groups of PEI strongly adsorb formaldehyde molecules through nucleophilic reactions, thus resulting in a negative frequency shift of the SAW sensor due to the mass loading effect. In addition, experimental results showed that the frequency shifts of the SAW devices are determined by thickness of PEI film, concentration of formaldehyde and relative humidity. The PEI/BC sensor coated with three layers of PEI as the sensing layer showed the optimal sensing performance, which had a frequency shift of 35.6 kHz for 10 ppm formaldehyde gas, measured at room temperature and 30% RH. The sensor also showed good selectivity and stability, with a low limit of detection down to 100 ppb.

Keywords: Polyethyleneimine (PEI); Bacterial cellulose (BC); SAW sensor; Formaldehyde gas; Bi-layer nanofilms.

1. Introduction

Formaldehyde is a colorless gas, extensively used in construction materials such as adhesives, building materials and coatings, as well as many household products [1,2]. Building materials, furniture, electrical appliances and many consumer goods release a certain concentration of formaldehyde, which becomes one of the main sources for indoor air pollution [3-5]. Long-term exposure to low levels of formaldehyde may cause headaches, memory loss, pulmonary edema and other symptoms. Whereas a short-term exposure to significant levels of formaldehyde can be fatal. Formaldehyde is classified as a carcinogen, and may cause leukemia and fetal malformation, especially affecting pregnant women and infants [5,6]. Considering the widespread uses of formaldehyde and its health hazards, accurate and fast detection of formaldehyde in indoor environments using cost-effective and portable sensors is urgently required. However, conventional methods using mass spectrometry and gas chromatography do not meet these needs as they require expensive equipment, professional operators and prolonged analysis time [8,9].

Different sensing methods for detection of harmful gases have been proposed, especially for highly hazardous formaldehyde gas [10-14]. For example, Tian et al. [15] developed a formaldehyde gas sensor using zeolitic imidazolate framework coated ZnO nanorods as the sensing layer, which improved the selectivity compared with the ZnO film sensors. Li et al. [16] prepared a resistive formaldehyde sensor using In_2O_3 nanofiber sensing layers prepared using an electrospinning technology.

Despite having a high sensitivity, it was reported to operate at an elevated working temperature of 300^{o}C [16]. Zhai et al. [17] used CdS nanoparticle-doped ZnO crystallites as the sensing layer to develop visible light-induced photoelectric sensors, which can detect formaldehyde efficiently, but the detection limit is only 10 ppm.

Acoustic wave and ultrasonic based sensors have been widely explored for the detection of hazardous gases, and among them, surface acoustic wave (SAW) sensors receive extensive attention because of their advantages of high sensitivity, short response time, low cost and suitability for wireless operation [18-22]. For example, Tang et al. [23] achieved excellent sensitivity, selectivity and stability for detection of ammonia using ZnO/SiO_2 bi-layer nanofilms.

Formaldehyde molecules are prone to reversible nucleophilic addition reactions with amine groups at room temperature [24]. The reaction mechanism is schematically shown in Fig. 1. The double bonds in the formaldehyde molecules have a sigma bond and a π bond. They are polar bonds, caused by the difference in electronegativity values of oxygen atom and carbon atom. The oxygen atom has a stronger ability to adsorb electrons, thus causing the electrons in the double bonds to be transported toward the oxygen atom. Therefore, the oxygen atom is negatively charged, whereas the carbon atom is positively charged. This makes carbon atoms (electrophiles) the primary target of nucleophiles. At the same time, a pair of electrons are present in the nitrogen atom in the amine group, which easily attack the electrophile as a nucleophile. This results in a nucleophilic addition reaction as shown in Fig. 1. The two bonds in the formaldehyde molecules then break up and form two

new covalent bonds. The reaction mechanism diagram shown in Fig. 1 indicates the reaction of the primary amino group with the formaldehyde molecules, and does not illustrate the reactions of the formaldehyde molecules with the secondary amino group and the tertiary amine group. This is because the formaldehyde molecules can only react with the secondary amines and tertiary amines at a high temperature or in the presence of catalysts [25]. It was reported that the secondary amino groups of PEI could adsorbs a small amount of formaldehyde molecules through a hydrogen bonding mechanism [26]. In addition, the reversibility of the above reaction ensures the repeatability of formaldehyde gas sensors based on such sensing materials [24,27].

Polyethylenimine (PEI) is a typical water-soluble polyamine, with a polar group (amino group) and a hydrophobic (vinyl) structure that allow it to be bound to different substances [28,29]. It has a wide range of applications in polymer dyes [30], papermaking [31], fiber modification [32] and biomedicine [33]. The PEI molecules contain a large number of amino groups, which have a good selectivity to adsorb the formaldehyde molecules and are suitable for detection of formaldehyde gas [34-36]. However, smooth surface of the conventionally prepared PEI has a low specific surface area and many agglomerated PEI particles, and thus has a low sensing performance for formaldehyde gas.

In this study, we propose to use network cellulose nanofilms to increase the specific surface areas of the PEI sensing films. The bacterial cellulose (BC) film used in this study is interwoven with filamentary fibers to form a hyperfine network structure [37], which has superior specific surface areas and porosity compared to the

other nanofilms [38]. Therefore, it is ideally used for improving the formaldehyde sensing properties of PEI films. The large specific surface area allows the sensing material to be well contacted with the targeted gas molecules. The hydroxyl groups of the BC can form strong hydrogen bonds with the amine groups of PEI [39], thus ensuring the uniform distribution of PEI on the BC films and avoiding the aggregation of PEI particles. In this paper, an ST-cut quartz SAW sensor, the surface of which treated with PEI/BC integrated sensing layer, was characterized for formaldehyde sensing in terms of its sensitivity, response and recovery time, selectivity and stability.

2. Experimental details

2.1 SAW resonator and bi-layer nano sensing layer

As shown in Fig. 2(a), the SAW resonator consists of interdigital transducers (IDTs, 30 pairs), reflective gratings (100 pairs), and nano-material-coated sensing films, which are deposited on ST-cut (42°75') quartz substrates (12 mm × 3 mm × 0.5 mm). The IDTs have a finger width of 4 μm and an aperture of 3 mm. The resonant frequency of the SAW resonator is ~200 MHz, as shown in the S21 spectrum in Fig. 2(b). The resonator exhibits a high quality factor with a value of 8966 and a low insertion loss with a value of -8.48 dB.

Preparation of the BC dispersion comprises the steps of using sucrose as a carbon source and corn syrup as a nitrogen source to ferment acetobacter xylinum in a medium at a mass ratio of 1:1. The oxygen-enriched air was introduced, the temperature was controlled at 30°C, and the pH of the culture solution was controlled

at 5.5. After 10 days of culture process, the produced BC was purified, e.g., pre-washed with deionized water, soaked in a 1 wt% NaOH solution at 80^{o}C for 20 min, and then rinsed with deionized water to obtain a purified BC content of 0.65 wt%. BC solution of 36.4 ml with a content of 0.65 wt% was diluted in 200 ml of deionized water. The mixture was mechanically stirred for 2 hrs and aged for 24 hrs to prepare a BC hydrosol with a concentration of 1 wt‰.

PEI of 1 ml in a 50 wt% aqueous solution (from Shanghai Aladdin Biochemical Technology Co., Ltd.) was diluted in 39 ml of deionized water at room temperature of 25^{o}C. The mixture was stirred for 2 hrs and aged for 24 hrs to obtain a PEI hydrosol with a concentration of 1.25 wt%.

When preparing the bi-layer nanofilm layer, the BC sol was firstly spin-coated onto the SAW device at 6000 rpm for 30 seconds, and then different layers of PEI films were prepared by multiple spin coating processes at 7000 rpm. The SAW device was placed in a 60^{o}C oven for 10 minutes after each step of spin coating. The preparation steps of the pure PEI membrane and the pure BC membrane are similar. Finally, the SAW resonator coated with the sensing film was connected to an oscillator circuit including amplifying and phase shifting units using gold wires to constitute a SAW-based formaldehyde gas sensor.

2.2 Sensing and characterization system

The experimental sensing system is shown in Fig. 3. The temperature and humidity of the experimental environment are controlled at 25^{o}C and 30% relative

humidity (RH), respectively. The entire sensing system consists of two closed compartments with an internal volume of 2 L and an external volume of 20 L, a constant temperature workbench, a hygrothermograph, a frequency counter and a digital source meter. The SAW device is placed inside the 2 L test chamber, which is placed inside the 20 L-test chamber.

During the experiments, the gaseous formaldehyde was obtained by injecting liquid formaldehyde into the evaporation station in the test chamber. The concentration of formaldehyde gas was controlled using a micropipette, through which the liquid formaldehyde was introduced into the test chamber. The amount of aqueous solution required for evaporation is extremely small, and the generated water vapor has little effect on the humidity change in the test chamber. For example, the experimental evaporation produces 20 ppm of formaldehyde gas, and the change of RH value in the test chamber is about 0.07%. After the formaldehyde solution was evaporated, the test chamber was returned to room temperature of 25^{o}C. Then the digital source meter and the frequency counter were switched on, and the 2 L test chamber was opened through a mechanical pulley to release the formaldehyde gas onto the surface of the SAW sensor. The frequency shift of the SAW gas sensor was monitored using a frequency counter (Agilent 53210A).

The volume of the gaseous formaldehyde (V_{gas}) is proportional to the volume of the test chamber (V_S) where the concentration of the gas (C) is the linear constant: [40]

$$V_{gas} = C \cdot V_s \qquad (1)$$

The relationship between the volume of the liquid formaldehyde (37 wt% in H_2O, from Shanghai Maclean Biochemical Technology Co., Ltd.) to the gaseous formaldehyde and its concentration can be obtained using ideal gas law and liquid volume equations [41].

$$n = \frac{PV_{gas}}{RT} = \frac{PCV_s}{RT} \qquad (2)$$

$$V_{liquid} = \frac{Mn}{\rho} = \frac{MPV_s}{R\rho} \cdot \frac{C}{T} \qquad (3)$$

where P (Pa) is the pressure, R ($J \cdot K^{-1} \cdot mol^{-1}$) is the ideal gas constant, V_{liquid} (L) is the volume of the liquid, M (g/mol) is the relative molecular mass of formaldehyde, ρ (g/ml) is the density of the formaldehyde solution, and T (K) is the temperature of the test environment. For the system we used, the values of M, P, Vs, R, and ρ are 30.03 g/mol, 101.325 kPa, 20 L, 8.31441 J/(mol·K) and 1.083 g/cm^3, respectively. The amount of formaldehyde solution required to set the concentration of formaldehyde gas can be obtained using equation (4):

$$V_{liquid} = 6.758 \cdot \frac{C}{T} \qquad (4)$$

Morphology of the sensing films on the surface of the resonator was characterized using a field emission scanning electron microscopy (FE-SEM, FEI-INSPECT F50). Surface functional groups of the BC and PEI were characterized using a Fourier transform infrared spectroscopy (FTIR, Nicolet IS 10, ThermoFisher Scientific). Changes of surface functional groups during the chemical reaction with formaldehyde gas were characterized using an *in situ* diffuse reflectance Fourier transform infrared (FTIR) spectrometer (DRIFT, Bruker Vertex 70).

3. Results and discussions

3.1 Characterization of bi-layer nanofilms

Fig. 4 shows SEM images of pure BC films, pure PEI films, and PEI/BC bi-layer nanofilms (with three layers of PEI). BC films have a large amount of ultrafine fibers, forming a porous and fibrous network structure. PEI film surface shows some non-uniform agglomerates but without apparent pores. The PEI/BC bi-layer nanofilms inherit the porous fiber network of the BC films, which facilitates the efficient penetration of gas inside the films.

FTIR analysis results of BC and PEI materials are shown in Fig. 5. The FTIR peaks of the BC material at 3332 and 1314 cm^{-1} are related to the stretching vibrations of -OH and C-OH, respectively [42]. The peaks at 2896, 1590, and 1029 cm^{-1} are caused by C-H stretching vibration, H-C-H deformation vibration, and C-N stretching vibration, respectively. The peak of the PEI material in the range of 3100-3500 cm^{-1} corresponds to the stretching vibration mode of the primary and secondary amine groups. The peaks at 2830, 2261, 1600, 1460, 1299, 1118, and 772 cm^{-1} are due to C-H, C≡C, C=C stretching vibrations, C-H internal bending vibration, C-N stretching vibration, C-C stretching vibration, and -(CH_2)- links, respectively [42]. The FTIR results shown in Fig. 1 verify the structures of BC and PEI. Moreover, the presence of hydroxyl groups on the BC and the amine groups on the PEI promotes strong hydrogen bonds, leading to uniform dispersion of PEI particles on the surface of the BC nanofilm, which can provide more adsorption sites for gas adsorption.

3.2 Gas sensing results and mechanism

Fig. 6(a) shows the frequency responses of the SAW sensors coated with pure BC films, pure PEI films, and PEI/BC bi-layer nanofilms, when exposed to 10 ppm of formaldehyde gas. The SAW sensor with the pure BC films has no apparent response to formaldehyde, indicating that the intrinsic BC is not sensitive to formaldehyde. After coating the PEI films on the surface of the BC nanofilms, the SAW sensor with three layers of PEI exhibits significant negative frequency shifts with a measured frequency shift of 35.6 kHz to 10 ppm of formaldehyde.

The gas sensing characterization results are summarized in Table 1. The frequency shift of the sensors increases significantly with the number of PEI layers. This can be attributed to the fact that the PEI/BC bi-layer nanofilm inherits the porous network structure of the BC nanofiber membrane and thus provides more attachment sites for the formaldehyde gas. The hydrogen bond formed between the hydroxyl group on the surface of BC and the amine group of PEI avoids the aggregation of PEI particles, ensures the uniform distribution of PEI on the BC films, and enhances the adsorption effect of formaldehyde gas. However, the response and recovery times also increase with the number of PEI layers. Although the adsorption sites are increased with the increases of PEI particles, gas molecules need a longer time to diffuse through the thicker layers. Moreover, when the BC thickness is increased when the PEI thickness is fixed, there is a little increase in the frequency shift. This may be attributed to the increase of the pores of the film, which reduces the aggregation of PEI particles. However, increasing the thickness of the BC increases the loading effect

of resonator and insertion loss. When the number of coated PEI layers exceeds three, the insertion loss of the SAW resonator exceeds -30 dB, and the quality of the vibration signal becomes very poor. Therefore, we will use the SAW devices with only three layers of PEI and a single layer of BC.

The response time of the sensor is defined as the time needed to reduce the resonant frequency shift to 90% of the maximum value, and the recovery time is the time needed to restore the resonant frequency shift to 10% of the maximum value. Fig. 6(b) shows the response and recovery characteristics of pure PEI membrane and PEI/BC bi-layer nanofilms with three layers of PEI SAW sensor when exposed to 10 ppm formaldehyde gas at 25^{o}C. Table 1 summarizes the response frequency shifts and response/recovery times of the SAW sensors coated with pure BC films, pure PEI films, and PEI/BC bi-layer nanofilms with different layers of PEI. Clearly the PEI/BC bi-layer nanofilm based SAW sensor coated with three layers of PEI layer exhibits the best sensitivity. Compared with the pure PEI membrane SAW sensor, the PEI/BC bi-layer nanofilm based SAW sensor has shorter response time and recovery time, e.g., for 10 ppm formaldehyde gas, the response time is reduced by 41% and the recovery time is reduced by 42% using the PEI/BC bi-layer nanofilms with three layers of PEI structure. This is because the fibrous network of the BC films enhances the penetration of gases from the films. Moreover, the presence of hydrogen bonds makes the PEI particles evenly distributed on the surface of the BC films, which facilitates the rapid attachment and removal of the formaldehyde molecules.

Fig. 7 shows results of dynamic responses of pure PEI films and PEI/BC bi-layer

nanofilms with three layers of PEI to different concentrations of formaldehyde between 100 ppb and 20 ppm. As can be seen in Fig. 7(a), the SAW sensors coated with the pure PEI sensing film do not apparently respond to formaldehyde when its concentration is below 2 ppm, whereas the presence of PEI/BC bi-layer nanofilms enhances the responses significantly. Fig. 7(b) summarizes the responses of the SAW sensors to various concentrations of formaldehyde. The slopes of the response curves for the sensor with PEI/BC bi-layer in the range of 1-2 ppm and 2-5 ppm are 5800 and 4100 Hz/ppm, respectively, whereas the slope for the sensor coated with pure PEI is only 240 Hz/ppm.

The previously reported PEI film based acoustic wave formaldehyde sensors are mostly based on film bulk acoustic resonator (FBAR) [28, 34-36], and there is no report available using the SAW sensor. Table 2 compares the sensitivity, response time and recovery time for the different types of formaldehyde gas sensors in literature. Due to their much higher operating frequencies, the sensitivity values of these FBAR sensors are much higher, however, their response/recovery times are much longer than those of the SAW sensors in this study.

We have further theoretically predicted the minimum detection limit of each sensor through the principle of the limit signal-to-noise ratio [43,44], simply because the set-up in this study could not be used to accurately measure the lowest concentration. The theoretical results are provided in details in the ***Supporting information*** (Fig. S1). The minimum detection limit of PEI/BC bi-layer nanofilm based gas sensor (2.3 ppb) is much lower than that of PEI sensing film (38.6 ppb).

In order to verify that the negative frequency shift of the SAW sensor in response to formaldehyde is truly caused by the adsorption of the gas by PEI, *in-situ* DRIFT measurements were performed. The PEI and BC samples were introduced to 10 ppm of formaldehyde along with dry air, then the DRIFT scanning spectra were obtained. Fig. 8 shows differential responses calculated using a reference spectrum. The formaldehyde group of the PEI sample shows C-O vibration peaks at 1067 and 1376 cm^{-1}, a C-H vibration peak at 2965 cm^{-1} and an O-H vibration peak at 3677 cm^{-1}, whereas no visible peaks are observed for the dry air group. On the other hand, the formaldehyde and dry air groups of the BC sample show no significant peaks. Therefore, it can be reasonably assumed that C-O, O-H, and C-H peaks are linked with new chemical bonds produced by adsorption of formaldehyde on the PEI layer. Therefore, the negative frequency shift response of the SAW sensor exposed to formaldehyde gas is the adsorption of formaldehyde gas by the PEI particles. As described in the introduction, the formaldehyde molecule undergoes a reversible nucleophilic addition reaction with the primary amino group in the PEI structure as explained in Fig. 1.

3.3 Influence of temperature and humidity on sensing performance

Humidity is one of the important interference parameters for SAW gas sensors. Therefore, we control the humidity of the testing chamber by using a saturated salt solution method [45], and investigated the effects of different RH levels on the sensing properties of PEI/BC bi-layer nanofilms with three layers of PEI SAW

sensors. Fig. 9(a) shows the sensing results of the SAW sensor exposed to 10 ppm formaldehyde gas in different chamber environments with RH values of 30%, 56%, and 84%, respectively. It can be observed that when the sensor is exposed to the same concentration of formaldehyde gas, its response increases as the relative humidity is increased. This can be attributed to the strong attraction of the amine groups of PEI and the hydroxyl groups of BC to H_2O molecules, which increase the mass loading on the SAW sensor. In addition, H_2O molecules enhance the adsorption of formaldehyde molecules by forming hydrogen bonds with formaldehyde molecules, which has also been reported in literature [46]. The sensor shows good responses at each RH level, and the response drift is less than 3%, which reveals the good stability of the sensor.

The SAW sensors are normally sensitive to temperature, and their dependency is generally determined by the temperature coefficient of frequency (TCF), which is known to be almost zero for ST-cut quartz crystal [14]. Fig. 9(b) shows the changes of the resonant frequency of the sensor with increasing temperature. The TCF of the PEI/BC bi-layer nanofilms with three layers of PEI SAW sensor is calculated to be ~-0.18 ppm/^{o}C, indicating that the ST-cut quartz substrate is not sensitive to temperature.

3.4 Selectivity and stability of SAW sensors

The selectivity of PEI/BC bi-layer nanofilms with three layers of PEI SAW sensor was further investigated, and the results are shown in Fig. 10(a). Different types of non-target gases were selected, including 100 ppm of reducing gas CO, H_2,

NH_3, H_2S, oxidizing gas NO_2, volatile gas benzene, toluene and ethanol, along with 10 ppm of target gas formaldehyde. The responses of the SAW device to CO, H_2, NH_3, H_2S, NO_2, benzene, and toluene are negligible, whereas the response to ethanol is weak compared to that to the formaldehyde (a significant shift in frequency with a value of 35.6 kHz), indicating that the sensor has an excellent selectivity for formaldehyde.

Long-term stability of the SAW sensor of PEI/BC bi-layer nanofilms with three layers of PEI was further tested by exposure of the device to 1-20 ppm of formaldehyde every 4 days within a period of one month. The responses of the sensors to the gas are very stable with the frequency shifts being less than 5% as shown in Fig. 10(b), indicating that the sensor has a good long-term stability.

4. Conclusions

A formaldehyde gas sensor based on ST-cut quartz SAW device is designed, fabricated and tested in this study, using PEI/BC bi-layer nanofilms as the sensing layer. The filamentous and fibrous network structure of the BC nanofilms provides increased attachment sites for the PEI, and the presence of hydrogen bonds prevents the significant aggregation of PEI particles. This significantly enhances the sensitivity of the SAW formaldehyde gas sensor and reduces response and recovery times. It was found that the PEI/BC bi-layer nanofilms with three layers of PEI SAW sensor shows an optimal sensing performance. It has a negative frequency shift of 35.6 kHz for 10 ppm formaldehyde gas at room temperature and 30% RH. It exhibits a good

selectivity to formaldehyde gas compared to the other types of gases such as CO, NO_2, benzene, toluene and ethanol. It also shows a good stability within a test period of one month. Studies have shown that the negative frequency shift of the sensor is caused by the nucleophilic addition reactions of the primary amino groups of PEI with the formaldehyde molecules, and the adsorption of formaldehyde molecules which caused the mass load change of the SAW sensor.

Acknowledgments

This study was supported financially by the Fundamental Research Funds for the Central Universities (A03018023801119), Engineering Physics and Science Research Council of UK (EPSRC EP/P018998/1) and UK Fluidic Network-Special Interest Group of Acoustofluidics, and Newton Mobility Grant (IE161019) through Royal Society and NFSC, and Royal Academy of Engineering: Research Exchange between UK and China.

References

[1] H. Chen, L. Sun, G. Li, X. Zou, Well-tuned surface oxygen chemistry of cation off-stoichiometric spinel oxides for highly selective and sensitive formaldehyde detection, Chem. Mater. 30 (2018) 2018-2027.

[2] F. Meng, H. Zheng, Y. Chang, Y. Zhao, M. Li, C. Wang, Y. Sun, J. Liu, One-step synthesis of Au/SnO_2/RGO nanocomposites and their VOC sensing properties, IEEE Trans. Nanotechnol. 17 (2018) 212-219.

[3] J. Flueckiger, F. Ko, K. Cheung, Microfabricated formaldehyde gas sensors, Sensors 9 (2005) 9196–9215.

[4] P. Chung, C. Tzeng, M. Ke, C. Lee, Formaldehyde gas sensors: A review, Sensors 13 (2013) 4468-4484.

[5] L. Wang, Y. Zhu, Q. Xiang, Z. Cheng, Y. Chen, J. Xu, One novel humidity-resistance formaldehyde molecular probe based hydrophobic diphenyl sulfone urea dry-gel: Synthesis, sensing performance and mechanism, Sens. Actuators B 251 (2017) 590-600.

[6] Y. Wang, C. Lee, C. Lin, L. Fu, Enhanced sensing characteristics in MEMS-based formaldehyde gas sensors, Microsyst. Technol. 14 (2008) 995–1000.

[7] X. Liu, Y. Zhang, X. Yang, Vitamin E reduces the extent of mouse brain damage induced by combined exposure to formaldehyde and PM 2.5, Ecotoxicol. Environ. Saf. 172 (2019) 33-39.

[8] L. Wang, Z. Wang, Q. Xiang, Y. Chen, Z. Duan, J. Xu, High performance formaldehyde detection based on a novel copper (II) complex functionalized QCM gas sensor, Sens. Actuators B 248 (2017) 820-828.

[9] S. Huang, W. Wei, L. Weschler, T. Salthammer, H. Kan, Z. Bu, Y. Zhang, Indoor formaldehyde concentrations in urban China: Preliminary study of some important influencing factors, Sci. Total Environ. 590 (2017) 394-405.

[10] L. Wang, J. Gao, J. Xu, QCM formaldehyde sensing materials: Design and sensing mechanism, Sens. Actuators B 293 (2019) 71-82.

[11] L. Wang, H. Xu, J. Gao, J. Yao, Q. Zhang, Recent progress in metal-organic

frameworks-based hydrogels and aerogels and their applications, Coord. Chem. Rev. 398 (2019) 213016.

[12] L. Wang, L, Y. Wu, J. Gao, J. Song, La doped AlPO-5: Enhenced NH_3 sensing properties, thermodynamic investigation and humidity-enhanced effect, J. Solid State Chem. 277 (2019) 54-60.

[13] L. Wang, X. Cha, Y. Wu, J. Xu, Z. Cheng, Q. Xiang, J. Xu, Superhydrophobic polymerized n-octadecylsilane surface for BTEX sensing and stable toluene/water selective detection based on QCM sensor, ACS Omega 3(2018) 2437-2443.

[14] L. Wang, Y. Yu, Q. Xiang, J. Xu, Z. Cheng, J. Xu, PODS-covered PDA film based formaldehyde sensor for avoiding humidity false response. Sens. Actuators B 255 (2018) 2704-2712.

[15] H. Tian, H. Fan, M. Li, L. Ma, Zeolitic imidazolate framework coated ZnO nanorods as molecular sieving to improve selectivity of formaldehyde gas sensor, Acs Sens. 1 (2016) 243-250.

[16] Z. Li, Y. Fan, J. Zhan, In_2O_3 nanofibers and nanoribbons: Preparation by electrospinning and their formaldehyde gas-sensing properties, Eur. J. Inorg. Chem. 21 (2010) 3348-3353.

[17] J. Zhai, D. Wang, L. Peng, Y. Lin, X. Li, T. Xie, Visible-light-induced photoelectric gas sensing to formaldehyde based on CdS nanoparticles/ZnO heterostructures, Sens. Actuators B 147 (2010) 234-240.

[18] Z. Cao, D. Xu, J.H. Jiang, J.H. Wang, H.G. Lin, C.J. Xu, X.B. Zhang, R.Q. Yu, Mimicking the olfactory system by a thickness-shear-mode acoustic sensor array, Anal. Chim. Acta 335 (1996) 117-125.

[19] Y. Mao, W.Z. Wei, J.H. Zhang, S.F. Zhang, X.Q. Rao, Real-time monitoring of formaldehyde-induced DNA-lysozyme cross-linking with piezoelectric quartz crystal impedance analysis, Anlyst 126 (2001) 1568-1572.

[20] I.E. Kuznetsova, B.D. Zaitsev, A.M. Shikhabudinov, O.M. Tsivileva, A.N. Pankratov, E. Verona, Acousto-electronic gas sensor based on mushroom mycelial extracts, Sens. Actuators B 243 (2017) 525-531.

[21] J. Devkota, P. Jagannath, D. Ohodnicki, SAW sensors for chemical vapors and

gases, Sensors 17 (2017) 801.

[22] A. Afzal, N. Iqbal, A. Mujahid, R. Schirhagl, Advanced vapor recognition materials for selective and fast responsive surface acoustic wave sensors: A review, Anal. Chim. Acta 787 (2013) 36-49.

[23] Y.L. Tang, Z.J. Li, J.Y. Ma, Y.J. Guo, Y.Q. Fu, X.T. Zu, Ammonia gas sensors based on ZnO/SiO_2 bi-layer nanofifilms on ST-cut quartz surface acoustic wave devices, Sens. Actuators B 201 (2014) 114–121.

[24] L. Feng, C. Musto, K. Suslick, A simple and highly sensitive colorimetric detection method for gaseous formaldehyde, J. Am. Chem. Soc. 132 (2010) 4046-4047.

[25] S. Saeung, V. Boonamnuayvitaya, Adsorption of formaldehyde vapor by aminefunctionalized mesoporous silica materials, J. Environ. Sci. 20 (2008) 379-384.

[26] W. Yu, Y. Wu, J.C. Chen, X.Y. Duan, X.F. Jiang, X.Q. Qiuab, Y. Li, Sulfonated ethylenediamine-acetone-formaldehyde condensate: preparation, unconventional photoluminescence and aggregation enhanced emission, RSC Adv. 6 (2016) 51257-51263.

[27] W. Hu, S. Chen, L. Liu, B. Ding, H. Wang, Formaldehyde sensors based on nanofibrous polyethyleneimine/bacterial cellulose membranes coated quartz crystal microbalance, Sens. Actuators B 157 (2011) 554-559.

[28] S. Song, D. Chen, H. Wang, Q. Guo, W. Wang, M. Wu, W. Yu, Film bulk acoustic formaldehyde sensor with polyethyleneimine-modified single-wall carbon nanotubes as sensitive layer, Sens. Actuators B 266 (2018) 204-212.

[29] J. Ma, S. Wang, D. Chen, W. Wang, Z. Zhang, S. Song, W. Yu, ZnO piezoelectric film resonator modified with multi-walled carbon nanotubes/polyethyleneimine bilayer for the detection of trace formaldehyde, Appl. Phys. A: Mater. Sci. Process. 124 (2018), 56.

[30] P. Karthika, S. Ganesan, M. Arthanareeswari, Low-cost synthesized organic compounds in solvent free quasi-solid state polyethyleneimine, polyethylene glycol based polymer electrolyte for dye-sensitized solar cells with high photovoltaic conversion efficiencies, Sol. Energy 160 (2018) 225-250.

[31] W. Shang, X. Qian, D. Yu, Preparation of a modified diatomite filler via polyethyleneimine impregnation and its application in papermaking, J. Appl. Polym. Sci. 135 (2018) 46275.

[32] L. Ma, G. Wu, Y. Zhu, X. Li, P. Han, G. Wang, G. Song, An effective non-covalent grafting approach to functionalize carbon fiber with polyethyleneimine in supercritical fluid to enhance the interfacial strength of carbon fiber/epoxy composites, Polym. Compos. 39 (2018) 2381-2389.

[33] S. Khetani, V. Kollath, V. Kundra, M. Nguyen, C. Debert, A. Sen, K. Karan, A. Sanati-Nezhad, Polyethylenimine modified graphene-oxide electrochemical immunosensor for the detection of glial fibrillary acidic protein in central nervous system injury, Acs Sens. 3 (2018) 844-851.

[34] W. Wang, D. Chen, H. Wang, W. Yu, M. Wu, L. Yang, Film bulk acoustic formaldehyde sensor with layer-by-layer assembled carbon nanotubes/polyethyleneimine multilayers, J. Phys. D: Appl. Phys. 51 (2018) 055104.

[35] D. Chen, L. Yang, W. Yu, M. Wu, W. Wang, H. Wang, Micro-electromechanical acoustic resonator coated with polyethyleneimine nanofibers for the detection of formaldehyde vapor, Micromachines 9 (2018) 62.

[36] J. Wang, D. Zhan, K. Wang, W. Hang, The detection of formaldehyde using microelectromechanical acoustic resonator with multiwalled carbon nanotubes-polyethyleneimine composite coating, J. Micromech. Microeng. 28 (2018) 015003.

[37] N. Tonouchi, T. Tsuchida, F. Yoshinaga, T. Beppu, S. Horinouchi, Characterization of the biosynthetic pathway of cellulose from glucose and fructose in acetobacter xylinum, Biosci. Biotechnol. Biochem. 60 (1996) 1337-1379.

[38] R. Olsson, M. Samir, G. Salazar-Alvarez, L. Belova, V. Ström, L. Berglund, O. Ikkala, J. Nogués, U. Gedde, Making flflexible magnetic aerogels and stiff magnetic nanopaper using cellulose nanofifibrils as templates, Nat. Nanotechnol. 5 (2010) 584-588.

[39] X. Wang, B. Ding, M. Sun, J. Yu, G. Sun, Nanofifibrous polyethyleneimine membranes as sensitive coatings for quartz crystal microbalance-based formaldehyde

sensors, Sens. Actuators B 144 (2010) 11 – 17.

[40] X. Li, Y. Chang, Y. Long, Influence of Sn doping on ZnO sensing properties for ethanol and acetone, Mater. Sci. Eng. C 32 (2012) 817-821.

[41] P. Atkins, P. Julio, D. Paula, Atkins' physical chemistry, Seventh edition higher, Education Press, 2006.

[42] C. Eaborn, The sadtler handbook of infrared spectra: edited by W.W. Simons, Heyden and Son, Ltd, London, J. Organomet. Chem. 171 (1979) 44.

[43] S. Ammu, V. Dua, S. Agnihotra, S. Surwade, A. Phulgirkar, S. Patel, S. Manohar, Flexible, all-organic chemiresistor fordetecting chemically aggressive vapors, J. Am. Chem. Soc. 134 (2012) 4533-4556.

[44] J. Li, Y. Lu, Q. Ye, M. Cinke, J. Han, M. Meyyappan, Carbon nanotube sensors for gas and organic vapor detection, Nano Lett. 3 (2003) 929-933.

[45] L. Greenspan, Humidity fixed points of binary saturated aqueous solutions, J. Res. Natl. Bur. Stand. 81A (1977) 89 – 96.

[46] Y. Dimitrova, Solvent effects on vibrational spectra of hydrogen-bonded complexes of formaldehyde and water: An ab initio study, Theochem. J. Mol. Struct. 391 (1997) 251–257.

Table 1. Summary of gas sensing results of BC, PEI and PEI/BC bi-layer nanofilms with different layers of PEI.

Sensing film	Formaldehyde concentration (ppm)	Frequency shift (Hz)	t_{res} (s)	t_{rec} (s)
BC	10 ppm	0	/	/
PEI	10 ppm	-2800	78	64
PEI/BC with one layer of PEI	10 ppm	-12400	41	31
PEI/BC with two layers of PEI	10 ppm	-19600	44	33
PEI/BC with three layers of PEI	10 ppm	-35600	46	37

Table 2. Comparison of sensitivity, response time and recovery time based on PEI films

acoustic formaldehyde sensor which have been reported.

Sensor	Operating frequency (MHz)	Sensing layer	Sensitivity (Hz/ppb)	tres (s)	trec (s)	Reference
FBAR	4500	PEI-modified SWNTs	1511	45.1	59.8	[28]
FBAR	4800	Layer-by-layer MWNTs/PEI	1900	36	45	[34]
FBAR	4400	PEI nanofibers	1216	25	60	[35]
FBAR	4300	Composite MWNTs/PEI	683	58	73	[36]
SAW	200	PEI/BC	5.8	31	28	This work

FBAR: film bulk acoustic resonator; SWNTs: single-wall carbon nanotubes; MWNTs: multiwalled carbon nanotubes.

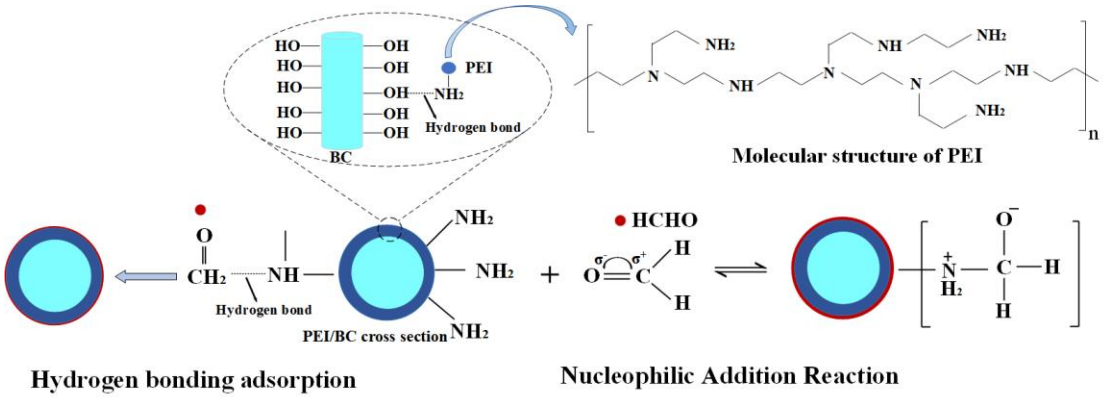

Fig.1. Schematic illustration of the reaction and adsorption mechanism of PEI/BC sensing membrane on formaldehyde gas.

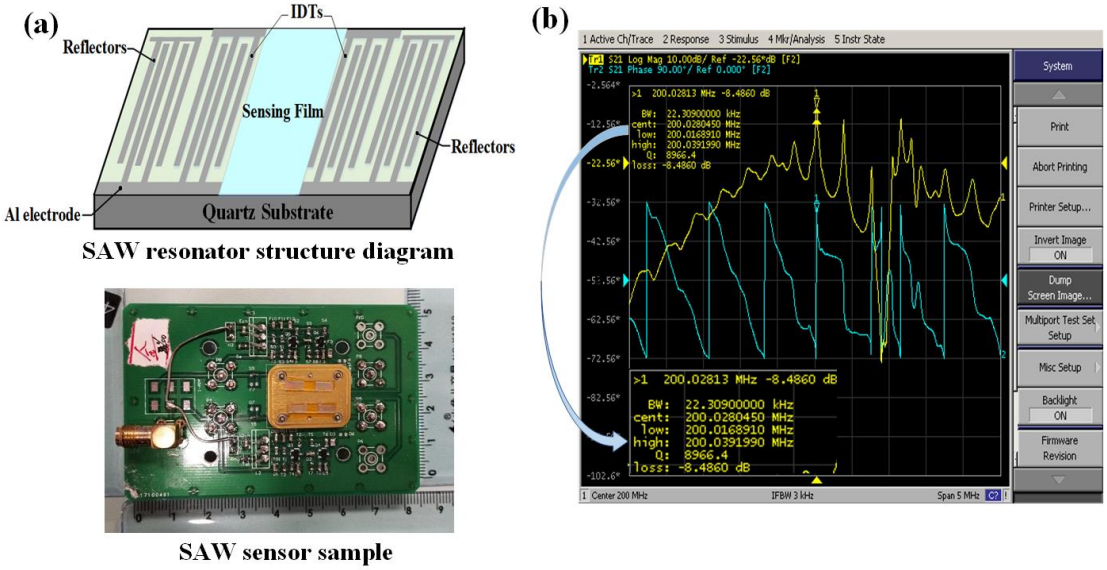

Fig.2. (a) SAW resonator structure and SAW sensor sample diagram and (b) a screen-copy of the obtained S-parameter during the detection.

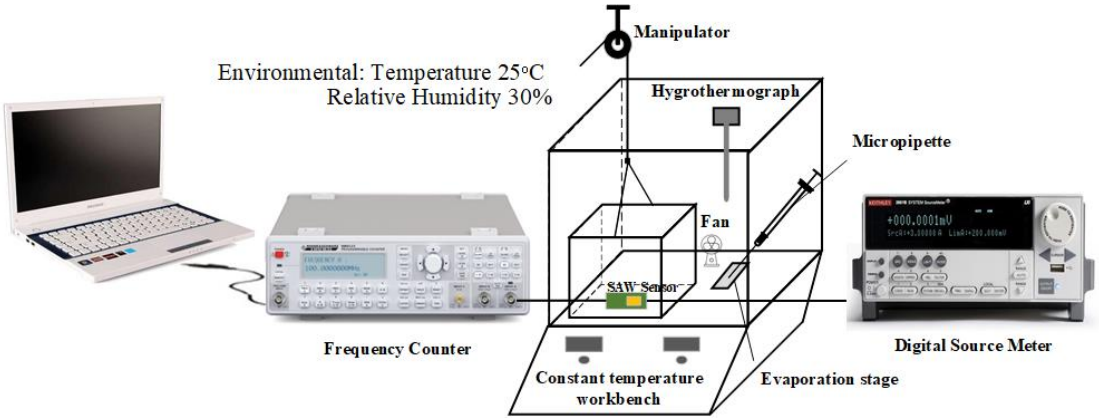

Fig.3. Schematic illustration of sensing system for formaldehyde gas.

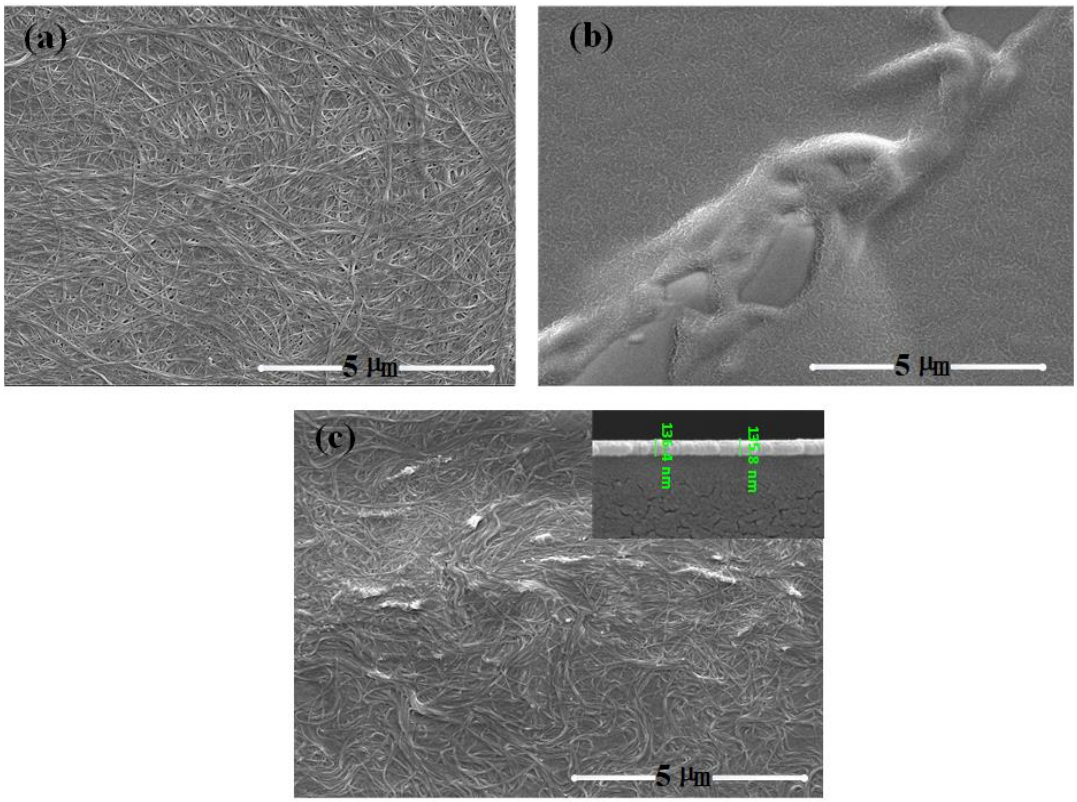

Fig.4. SEM images of (a) BC nanofilms; (b) PEI nanofilms; and (c) PEI/BC bi-layer nanofilms with three layers of PEI.

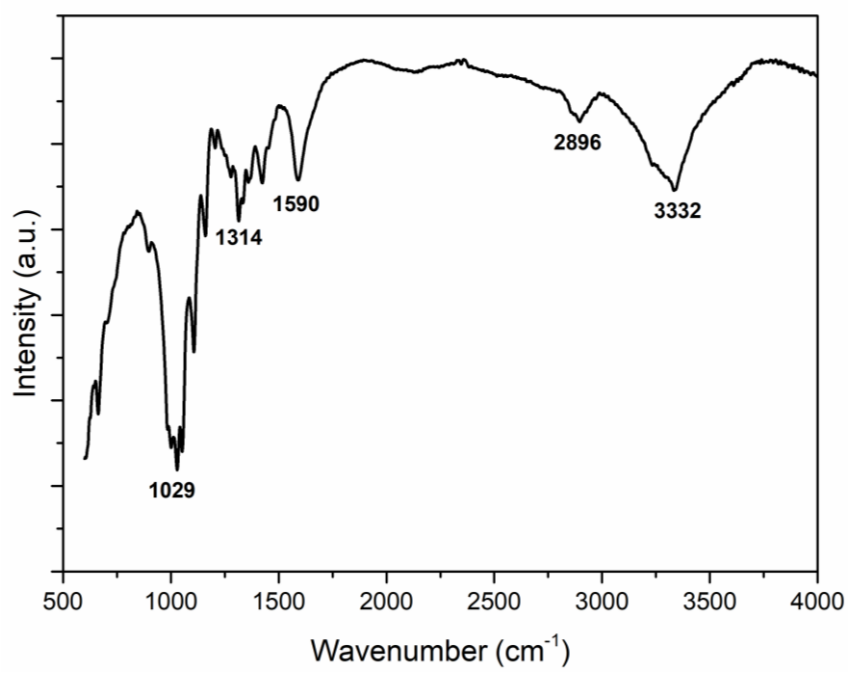

(a)

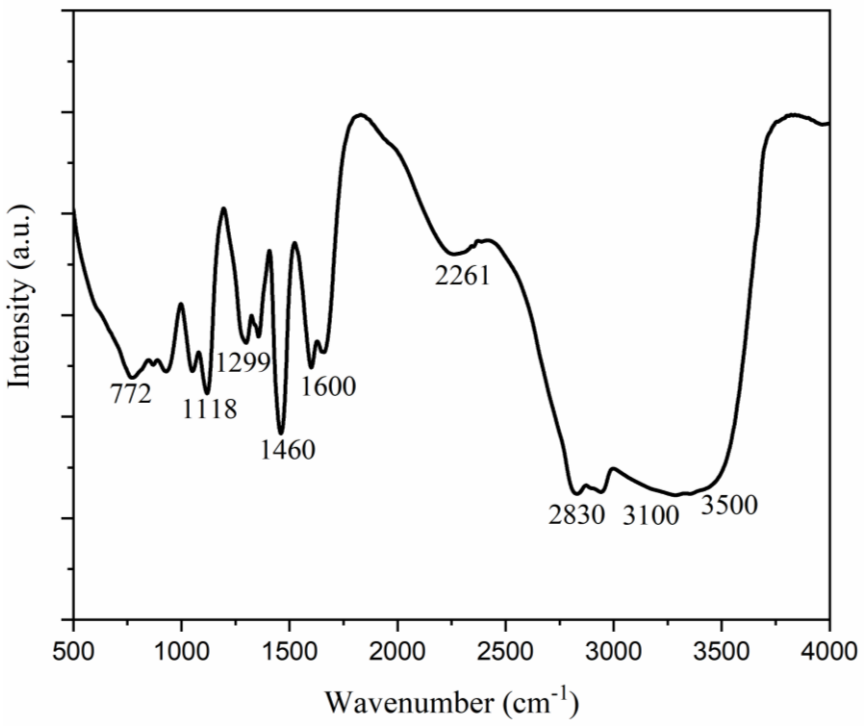

(b)

Fig.5. FTIR spectra of BC (a) and PEI (b) showing their surface groups.

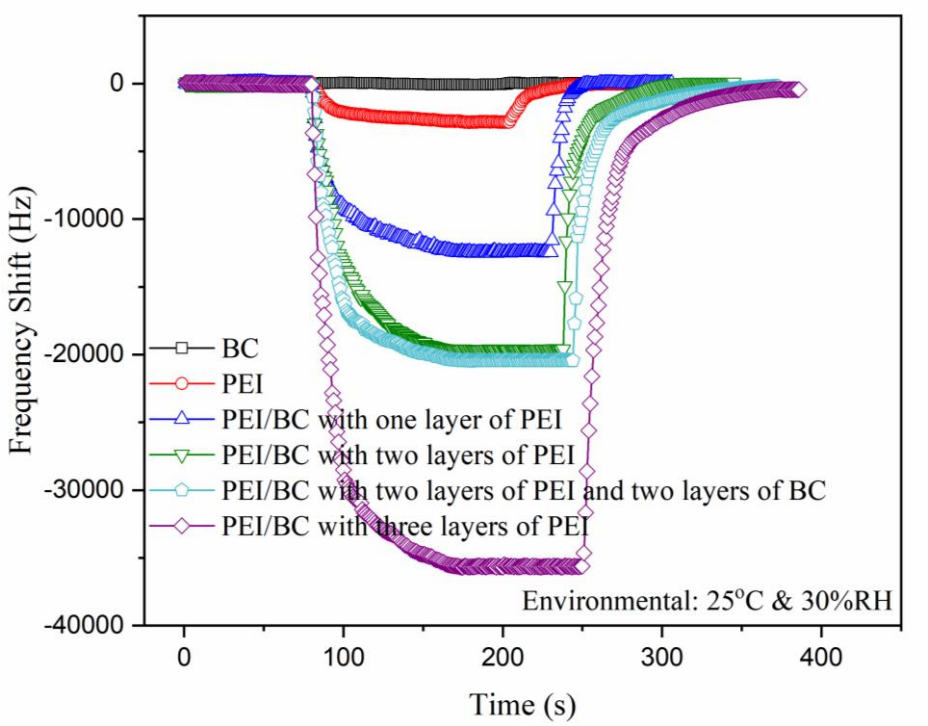

(a)

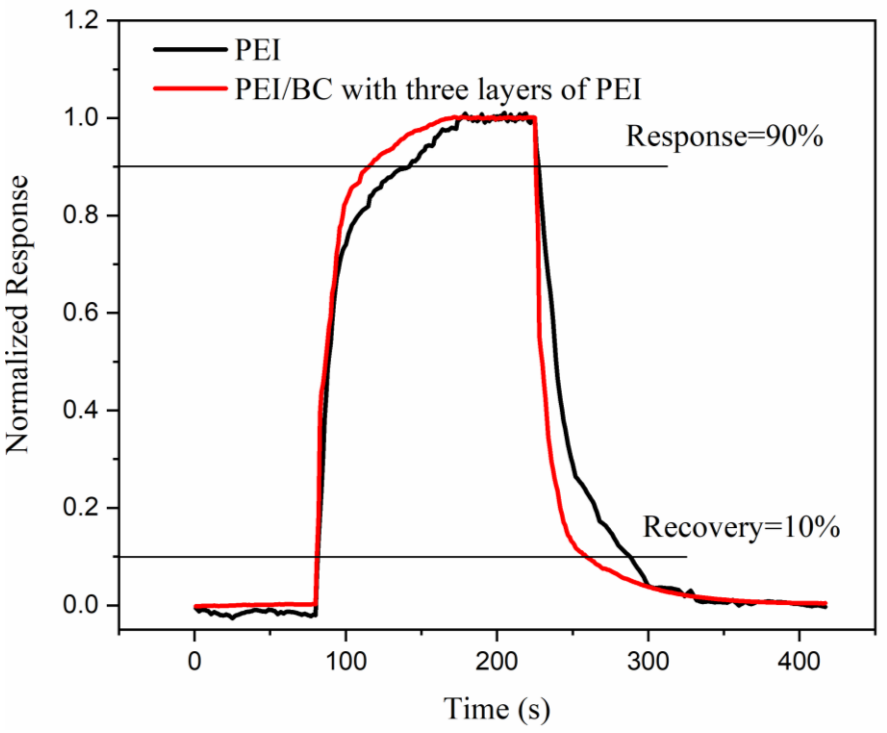

(b)

Fig.6. (a) Responses of SAW sensors coated with different sensing membranes to 10 ppm formaldehyde gas; and (b) normalized dynamic response of SAW sensors with PEI film and PEI/BC bi-layer nanofilms with three layers of PEI exposed to 10 ppm formaldehyde gas.

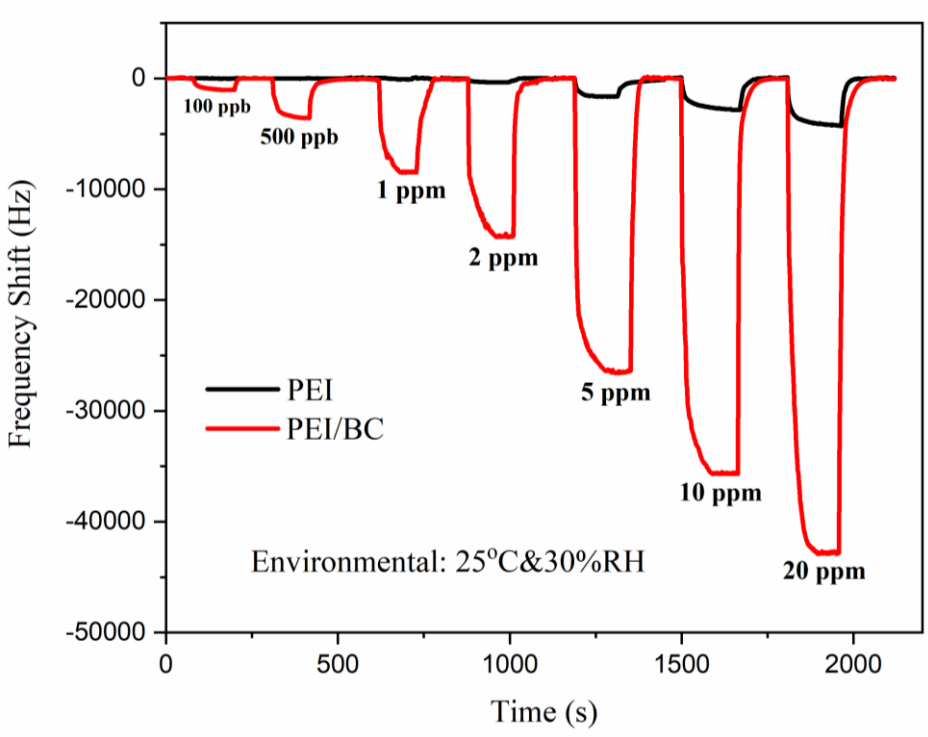

(a)

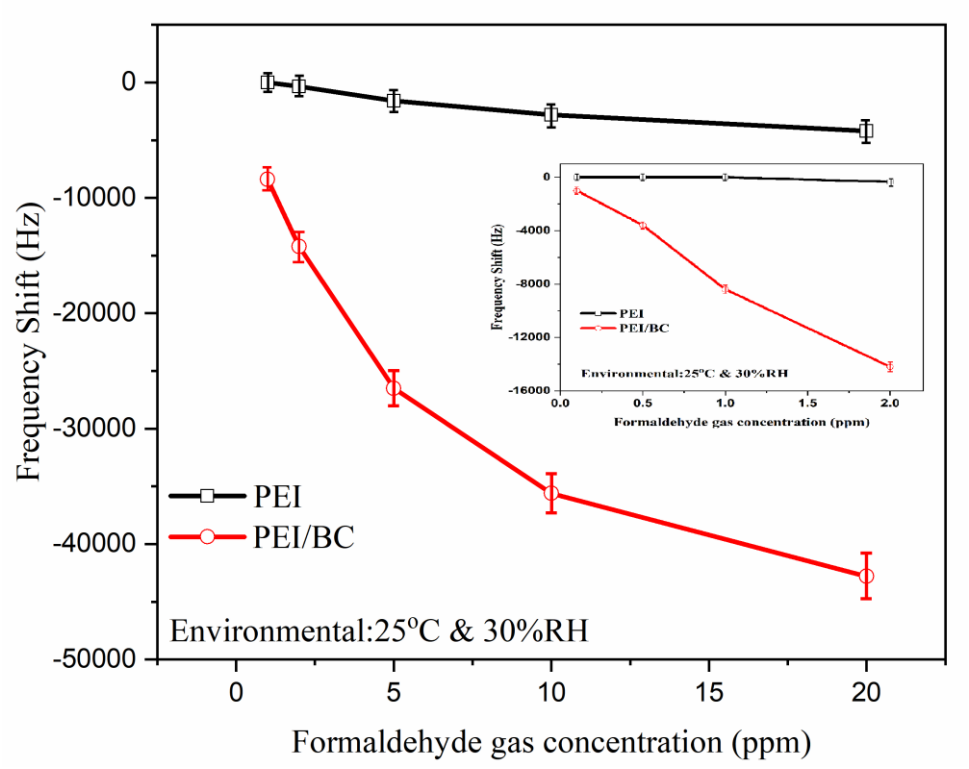

(b)

Fig.7. (a) Dynamic responses of PEI nanofilms and PEI/BC bi-layer nanofilms with three layers of PEI SAW sensors to different concentrations of formaldehyde gases; and (b) the curve of responses with concentration of formaldehyde gas.

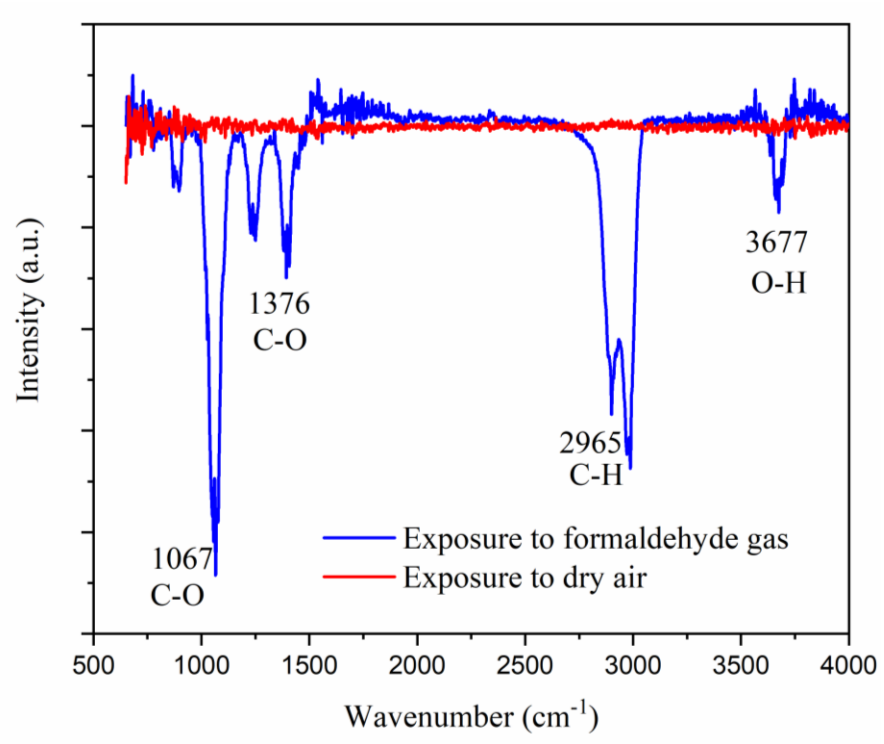

(a)

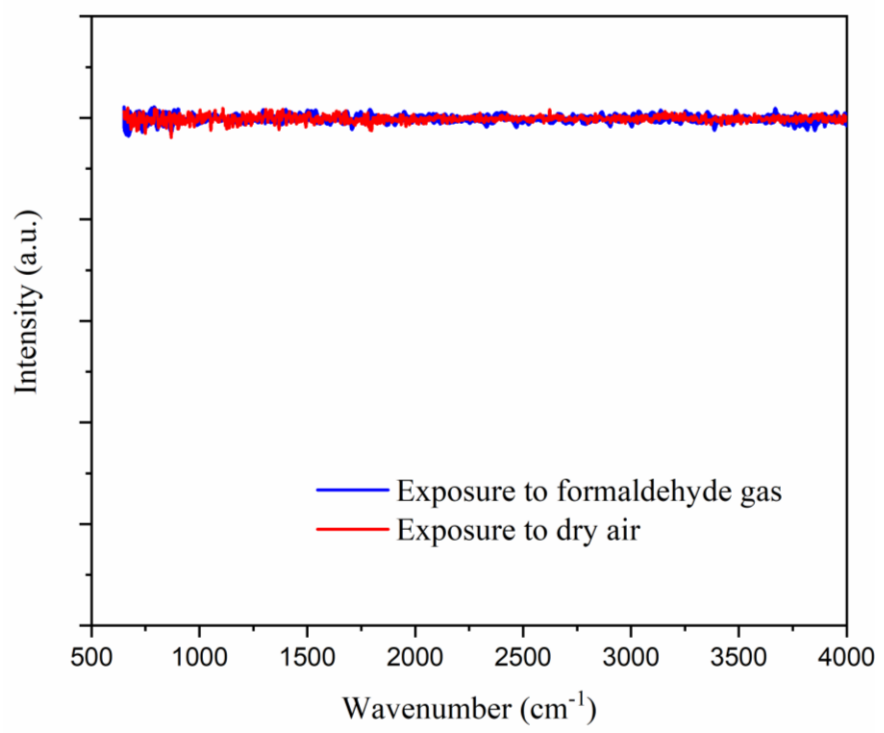

(b)

Fig.8. ***In-situ*** **DRIFT detection results of (a) PEI sample; and (b) BC sample. The cruves was obtained after the reference spectrum before exposure to gas was removed from the response spectrum after exposure to gas.**

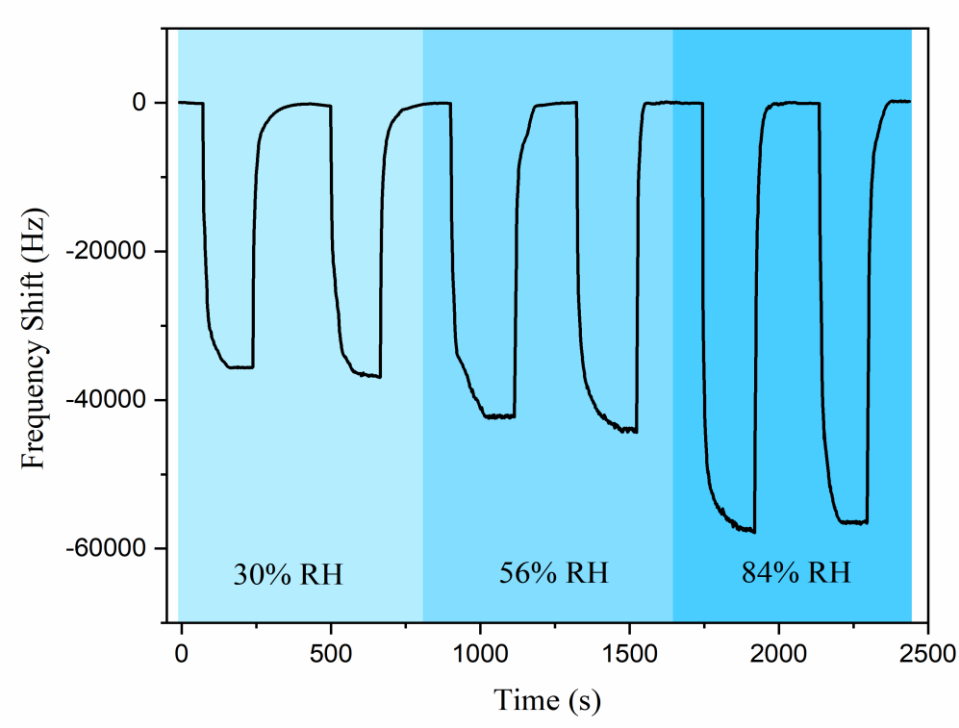

(a)

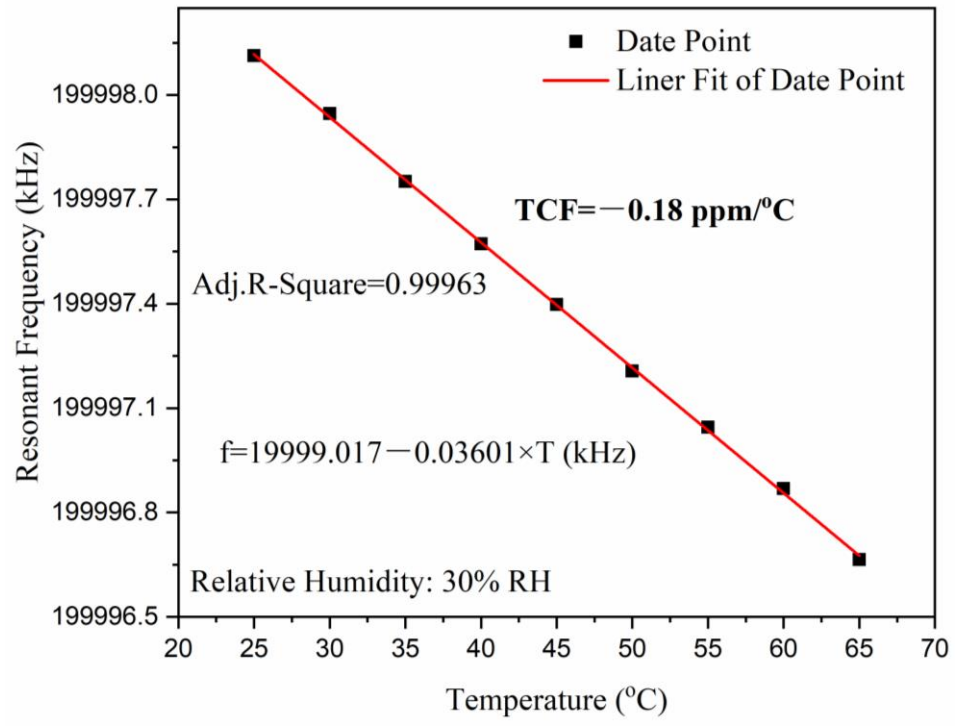

(b)

Fig. 9. (a) Response-recovery curve of PEI/BC bi-layer nanofilms with three layers of PEI SAW sensors to 10 ppm formaldehyde gas at the same room temperature of 25°C and different relative humidity levels; (b) The relationship between resonant frequency and temperature of PEI/BC bi-layer nanofilms with three layers of PEI SAW sensors.

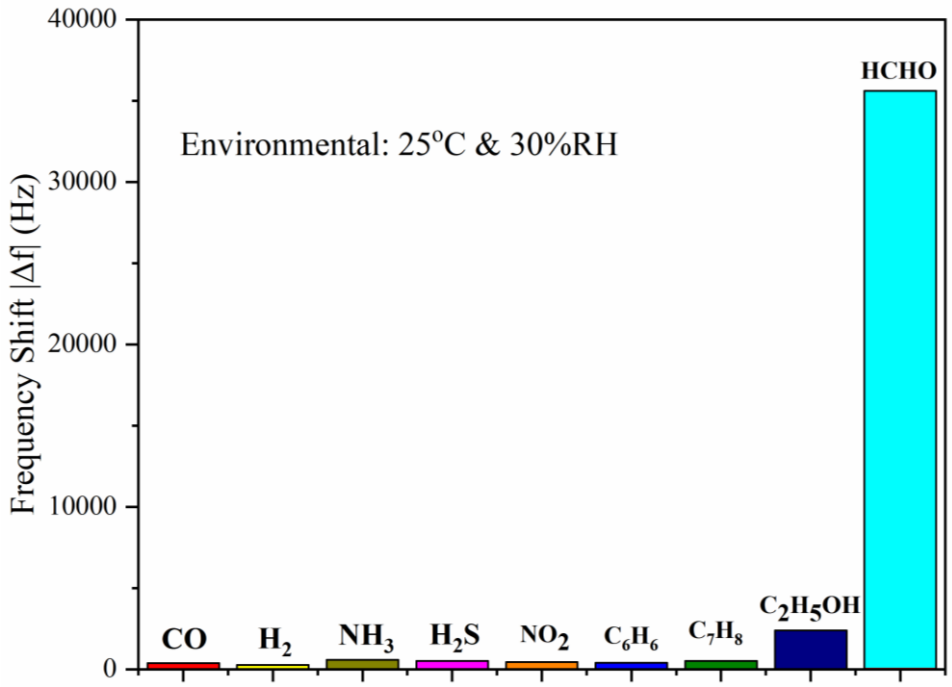

(a)

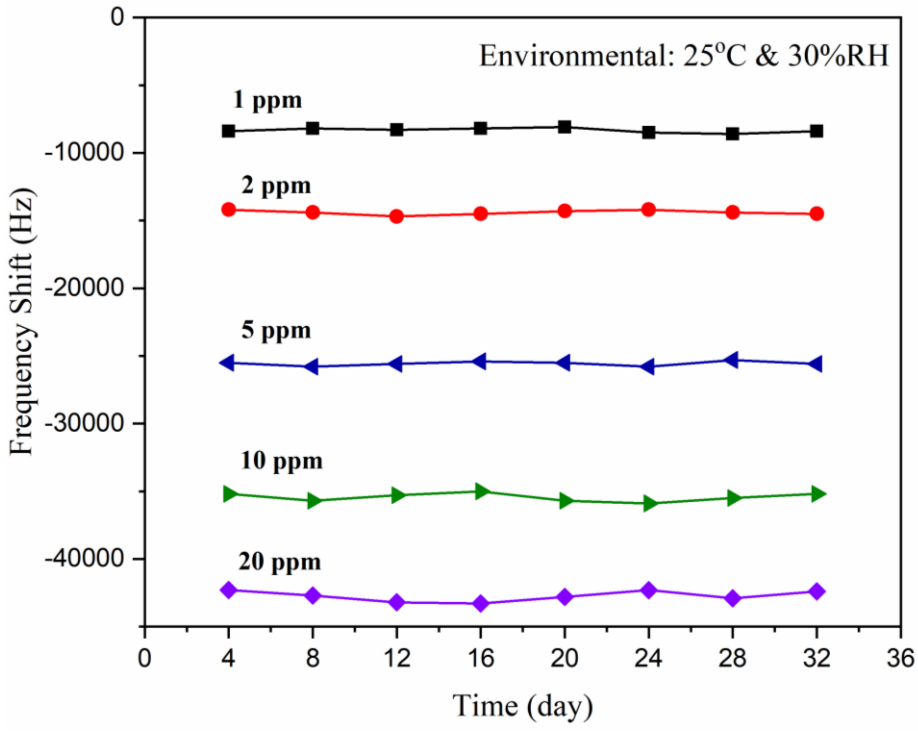

(b)

Fig.10. (a) Frequency shift of PEI/BC bi-layer nanofilms with three layers of PEI SAW sensors exposed to 100 ppm of various reducing and volatile gases and 10 ppm of formaldehyde gases; (b) Frequency shift of the sensors exposed to different concentrations of formaldehyde gas every four days for one month.